International Journal of Pharmaceutics 413 (2011) 93–102

Contents lists available at ScienceDirect

International Journal of Pharmaceutics

journal homepage: www.elsevier.com/locate/ijpharm

Inhalation performance of pollen-shape carrier in dry powder formulation: Effect of size and surface morphology

Meer Saiful Hassan, Raymond Lau*

School of Chemical and Biomedical Engineering (SCBE), Nanyang Technological University (NTU), Singapore

ARTICLE INFO

Article history:
Received 15 December 2010
Received in revised form 8 March 2011
Accepted 15 April 2011
Available online 21 April 2011

Keywords:
Dry powder inhalation
Pollen-shape carrier particles
Drug mixing ratio
Emitted dose
Fine particle fraction
Particle size
Surface morphology

ABSTRACT

In a previous study, pollen-shape drug carriers are compared with traditional carriers at different drug mixing ratios and flow rates. It is found that pollen-shape drug carriers can deliver large amount of drug particles and reduce drug losses especially at low flow rates and high drug mixing ratios. In this study, the effect of size and surface morphology of pollen-shape carriers on drug delivery performance is assessed. Pollen-shape carrier particles having various sizes and surface asperities are synthesized. Budesonide (Bd) is used as the model drug. The drug delivery performances of the pollen-shape carrier particles are investigated using an Andersen Cascade Impactor (ACI) equipped with a Rotahaler® at gas flow rates of 30 and 60 L/min. Three drug mixing ratios are considered. While an increase in the carrier particle size has a mild improvement on the ED, it significantly improves the FPF. A sparse surface asperity has negligible effect on the ED at low flow rates but it improves the FPF compared to a dense surface asperity under all experimental conditions.

1. Introduction

Dry powder inhalation requires the drug particles to have an aerodynamic size range of 1–5 μm (Gonda, 2004; Louey et al., 2004a). Particles in this size range experience significant interparticle forces and are difficult to disperse by air flow (Visser, 1989). A common practice to improve the drug delivery efficiency is to blend the fine drug particles physically with large carrier particles. In the blend, drug particles are attached onto the surface of the large carrier particles. The formulation blend is introduced to the patient through inhalation using different types of inhaler devices. The drug particles will be separated from the carrier surface during inhalation and delivered to the lower airways (Islam et al., 2004). Carrier particles, being relatively large, mostly deposit in the initial airways and swallowed eventually.

Carrier particles that are too small give limited improvement to the dispersion of the formulation while carrier particles that are too large pose high possibility of premature deposition in the upper airways by inertial impaction. Dry powder inhalation studies in the literature cover a wide carrier particle size range 8–220 μm. Diverse results on the efficient carrier particle size range are found under various inhalation systems, carrier materials and flow parameters (Begat et al., 2004; French et al., 1996; Guchardi et al., 2008; Heng et al., 2000; Islam et al., 2004; Kassem and Ganderton, 1990; Louey et al., 2004b, 2003; Podczeck, 1999; Srichana et al., 1998; Zeng et al., 2000, 1999). Nonetheless, the most efficient carrier particle size is commonly reported as 30–90 μm (Flament et al., 2004; Iida et al., 2001; Kawashima et al., 1998; Larhrib et al., 2006, 2003a,b, 1999; Young et al., 2005; Zeng et al., 2001). A number of studies found an increase in respirable fractions of the drug particles with a decrease in carrier particle size (Islam et al., 2004; Steckel and Müller, 1997). In contrast, a study reports that large carriers of 90–125 μm can provide higher respirable fractions than 38–75 μm carriers because of the lower interparticle forces among the large carrier particles (French et al., 1996). It is possible that the variations in these literature studies are caused by the presence of fine particles in the carrier particle samples which are difficult to separate by normal separation methods. Drug loading, dispersibility and detachment behavior of the drug–carrier mixture are affected substantially by the fine particles. When decantation method is used to minimize the presence of fines in the carrier particles, no significant difference is found in the drug respirable fractions using carrier particles in a size range of 45–190 μm (Islam et al., 2004).

Surface morphologies of the carrier particles have important effect on the attachment and detachment of the drug particles. For efficient drug delivery, the drug particles need to be loaded and liberated efficiently from the carriers. Most of the pharmaceutical grade carrier particles for dry powder inhalation have a certain extent of surface roughness. Rough surfaces tend to have more binding sites to facilitate the attachment of drug particles (Kawashima et al., 1998; Larhrib et al., 2006) and to improve

* Corresponding author. Tel.: +65 63168830; fax: +65 67947553.
E-mail address: wmlau@ntu.edu.sg (R. Lau).

0378-5173/$ – see front matter © 2011 Elsevier B.V. All rights reserved.
doi:10.1016/j.ijpharm.2011.04.033

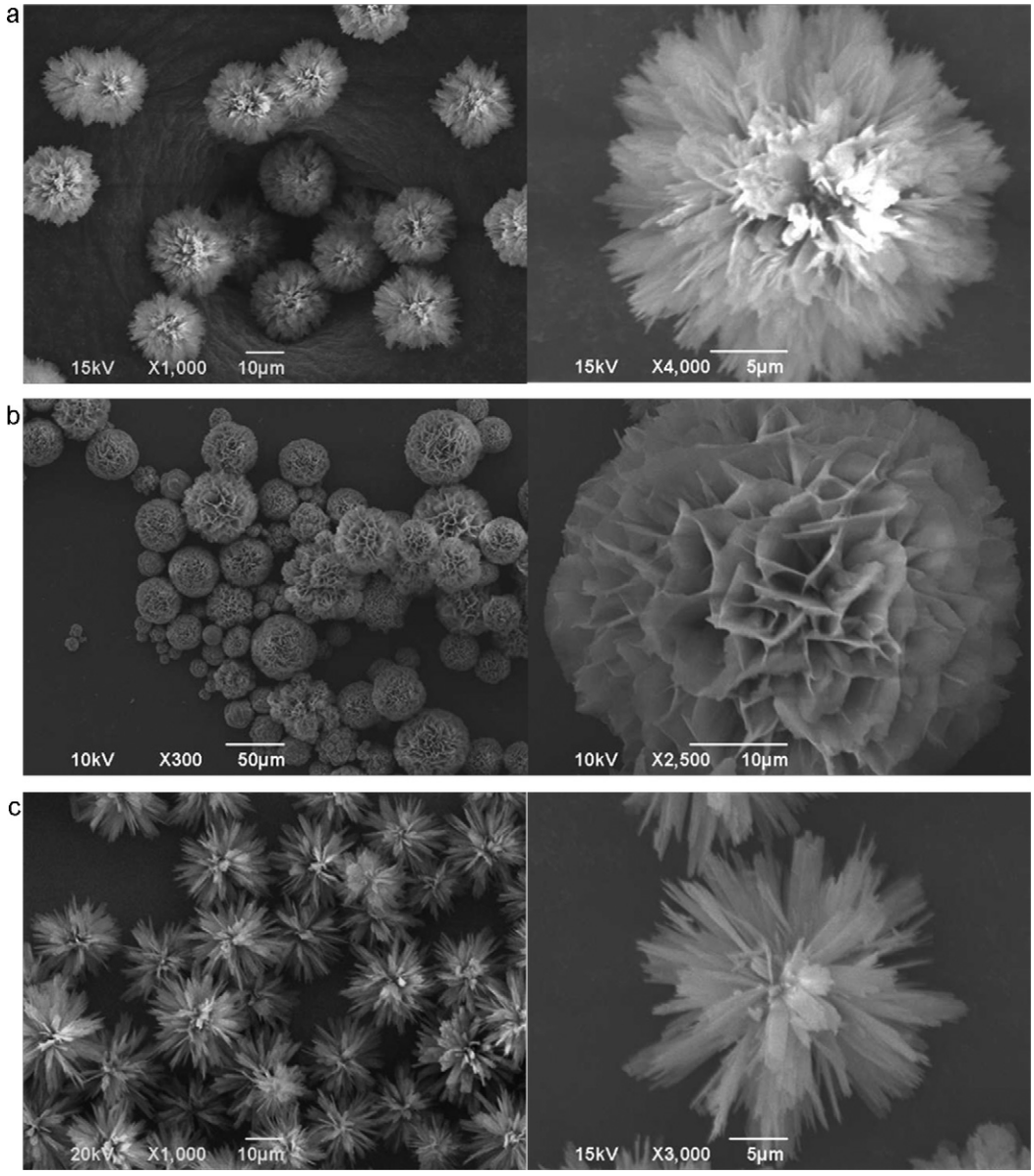

Fig. 1. The SEM image of HA particles produced by using (a) PSS-50 g/L and urea-0.5 M, at 180 °C (HA-1), (b) PSS-40 g/L and urea-0.5 M, at 120 °C (HA-2) and (c) PSS-30 g/L and urea-0.5 M, at 200 °C (HA-3).

the blend homogeneity and stability (Flament et al., 2004; Zeng et al., 2000). Rough surfaces also have low interparticle interactions because the contact surface area is small and the interparticle distance is relatively large (Broadhead et al., 1994; Dolovich, 2001; Gonda, 1996; Li et al., 2006; Niven et al., 1994; Philip et al., 1997; Singh and Waluch, 2000). It is also reported that a small degree of crevices on the carrier particles can increase the drug respirable fractions (Iida et al., 2001, 2004; Kawashima et al., 1998; Mumenthaler et al., 1994).

It is found in previous studies that pollen-shape large carrier particles can be a good candidate as drug carriers for dry powder inhalation. The pollen-shape surface morphology reduces the particle–particle interactions and improves the flowability (Hassan and Lau, 2010a,b,c). Better flow and aerosolization behaviors and drug attachment are observed in pollen-shape carriers compared to traditional lactose carriers. In this study, effect of carrier particle size and surface morphology on the drug attachment behavior and *in vitro* aerosolization and deposition properties of Budesonide (Bd) blended with pollen-shape hydroxyapatite (HA) carrier particles are investigated. Comparisons are made using three different drug mixing ratios and at inhalation flow rate of 30 and 60 L/min.

2. Experimental

2.1. Preparation of HA

Pollen-shape hydroxyapatite (HA, $Ca_5(PO_4)_3(OH)$) particles are synthesized by hydrothermal reaction under different reaction conditions. The synthesis procedure is following Wang et al. (2009). 30 mL of 0.02 M potassium dihydrogen phosphate (KH_2PO_4, Merck, Singapore) is mixed with 50 mL of 0.02 M calcium nitrate tetrahydrate ($Ca(NO_3)_2{\cdot}4H_2O$, Sigma–Aldrich, Singapore). A fixed amount of poly(sodium-4-styrene-sulfonate) (PSS, Aldrich, Singapore) and urea(1st Base, Singapore) are then added to the KH_2PO_4 and $Ca(NO_3)_2{\cdot}4H_2O$ mixture in sequence. Sufficient time of gentle stirring is provided to dissolve all the urea. The urea concentration in the final solution mixture is maintained at 0.5 M. The mixture is then kept in an oven at a constant temperature. The PSS con-

centration and oven temperature will govern the size and surface morphology of the HA particles synthesized. HA-1 is synthesized using a PSS concentration of 50 g/L and an oven temperature of 180 °C, HA-2 using a PSS concentration of 40 g/L and an oven temperature of 120 °C and HA-3 using a PSS concentration of 30 g/L and an oven temperature of 200 °C. A reaction time of 6 h is used for all the synthesis. After the hydrothermal reaction, the precipitated product is collected by centrifugation, washed several times and then dried at 70 °C. To remove particles with unusual size, particle products are sieved with appropriate sieve plates.

2.2. Particle size and shape

Particle size distribution of the three HA samples are measured by laser diffraction using a Mastersizer 2000 (Malvern Instruments Ltd., Malvern, Worcestershire, UK). Dispersed particle samples in 1% IPA solution in distilled water are fed into the sampling chamber of the particle sizer. A sonicator installed in the sampling chamber is used to help dispersing the particles properly in the solution. A minimum of three measurements are performed for each sample. The laser diffraction data obtained are expressed in terms of particle diameter at 10%, 50% and 90% of the volume distribution. The homogeneity of the particle sample can be represented by the span of the volume distribution (Li et al., 2004)

$$\text{Span} = \frac{d(90\%) - d(10\%)}{d(50\%)} \quad (1)$$

Scanning electron microscope (SEM) (JSM-5600, JEOL, Tokyo, Japan) is also used to characterize the size distribution, shape and surface morphology of the samples. Dry powder of each sample is dispersed onto a carbon tape that is attached onto a metal stub. Before examining the sample under SEM, platinum will need to be coated on the particle surface under an argon atmosphere (JFC-1600, JEOL, Auto Fine Coater, Tokyo, Japan) with a current of 20 mA for 60 s. SEM images taken at various locations of the carbon tape will be used to obtain the geometrical size distribution of the particles. A minimum sample size of two hundred is considered for each size distribution. Surface morphology of the particles is also assessed qualitatively based on the SEM images.

2.3. Powder density

The powder density of each HA sample can be characterized by their respective bulk (ρ_{bulk}) and tap (ρ_{tap}) densities. Based on the experimental method described in Shi et al. (2007), 100 mg of a powder sample is placed into a 1 mL micro-syringe tube. The bulk density is determined based on the powder volume before any tapping. The tube is then tapped against a tabletop by hand at a rate of about 4 Hz until no noticeable change in the powder volume. The tap density is then determined based on the tapped powder volume.

2.4. Crystalline structure

X-ray diffraction (XRD) is performed to determine the crystalline structure of the HA samples. A thin layer of the powder sample is placed onto a sample holder. The sample holder is then inserted into LabX-Shimadzu XRD6000 diffractometer (Shimadzu Corporation, Kyoto, Japan) using Cu Kα as the X-ray source (λ = 1.5406 Å). The XRD setting is fixed at a scan rate of 0.5/min, voltage of 40 kV, current of 40 mA, and step size of 0.02 for all measurements.

2.5. Moisture content

Moisture adsorbed on the surface of the particles is measured by thermogravimetric analysis (TGA, Diamond TG/DTA, Perkin Elmer, MA, USA). 1–2 mg of each sample is used for TGA measurement. Measurement is performed from 25 °C to 125 °C at a heating rate of 10 °C min^{-1} under a nitrogen atmosphere.

2.6. Specific surface area

The BET surface area of each HA sample is measured. Each sample is first dried at 80 °C for 24 h in Autosorb® Degasser (Quantachrome Instruments, FL, USA) under nitrogen. The surface area of the sample is then measured in an Autosorb® 6B (Quantachrome Instruments, FL, USA) surface analyzer with nitrogen adsorption method.

2.7. Blending of HA particles with Bd

Budesonide (Bd) (Sigma, Singapore) is chosen as the model drug. A REAX top mixer (Heidolph, Kelheim, Germany) is used to mix the drug and the HA carriers. Carrier to drug mixing ratios of 2:1, 10:1, and 45:1 are used. Each blend weights 100 mg and is mixed under 1000 rpm for 15 min.

2.8. Drug content and content uniformity

Average drug content and content uniformity of all the blends are measured by analyzing the quantity of Bd. 5 mg of each blend is taken and dissolved in a fixed amount of solvent. The solvent is a mixture of 2% nitric acid (Fluka, Singapore) with ethanol (Merck, Singapore) in a volume ratio of 3:1. The solution with dissolved sample is examined using a UV spectrophotometer (Shimadzu Corporation, Kyoto, Japan) with a wavelength of 250 nm. Measurement is done in triplicate. The content uniformity for the mixture is estimated from the coefficient of variance (CV). The CV is defined as the ratio of the standard deviation of the drug content to the average drug content in the samples.

2.9. In vitro aerosolization and deposition properties

An eight-staged Anderson cascade impactor (ACI) (Copley Scientific Limited, Nottingham, UK) is used for the *in vitro* aerosolization and deposition study. 1% (w/v) solution of silicon oil in hexane is coated on all the impaction plates in the ACI to prevent particle bounce and re-entrainment. A Rotahaler® (Glaxo, UK) device is used to introduce the Bd blends into the ACI. A hard gelatin capsule (Gelatin Embedding Capsules, size 4, 0.25 cm^3, Polysciences, Inc., PA, USA) is loaded with 10 ± 0.3 mg of a blend before introducing into the Rotahaler®. Two air flow rates of 30 L/min and 60 L/min are used. In order to maintain the same inhalation volume, an actuation time of 4 s and 8 s are used for 60 L/min and 30 L/min, respectively. The amount of particles collected in each section of the ACI is determined by extracting the particles using the same solvent used for the blend homogeneity test. Experiments on each blend are repeated three times.

The primary parameters to quantify the aerosolization and deposition properties of the blend are emitted dose (ED) and fine particle fraction (FPF). ED is defined as the mass percentage of particles delivered from the inhaler and FPF is defined as the amount of the particles deposited in stage 2 or lower in the cascade impactor for 30 L/min and stage 0 or lower for 60 L/min (particles <5.8 μm).

Table 1
Physical characteristics of the HA samples.

Characteristics	HA-1	HA-2	HA-3
Average diameter (SEM) (μm)	25.9	48.6	27.1
SD (μm)	2.49	10.21	4.02
d(50%) (μm)	26.6	45.9	24.8
d(10%) (μm)	19.1	25.9	15.1
d(90%) (μm)	36.9	85.9	41.0
Span	0.67	1.31	1.04
ρ_{bulk} (g/cm^3) (n = 0)	0.267	0.215	0.105
ρ_{tap} (g/cm^3) (n = 2500)	0.386	0.289	0.218
Specific surface area (m^2/g)	17.45	17.1	20.83

3. Results and discussions

3.1. Particle characteristics

Particle tip to tip distance is taken as the particle size for SEM size measurement. Since the size distributions measured from the SEM images are number-weighted while the size distributions measured from laser diffraction measurement are volume-weighted, the SEM size distributions are converted to volume-weighted distribution for comparison. For the conversion of number-weighted size distribution to volume-weighted size distribution, the pollen-shape particle volume is estimated to be the same as a sphere having the same diameter. Therefore, the SEM measured sizes are slightly higher than d(50%) of the laser diffraction measured size. Nonetheless, the size distribution can be considered uniform since the span of all the HA particles are close to 1 (Li et al., 2004).

Physical properties of the HA particles synthesized in this study are presented in Table 1. The SEM images of the HA particles and the respective SEM measured size distributions are presented in Figs. 1 and 2, respectively. The SEM image in Fig. 1 shows that HA-1 and HA-2 particles have a petal-like surface morphology with significantly distinct size range. On the other hand, HA-3 particles have a needle-like surface morphology and a geometric size range similar to HA-1 particles. Similar specific surface area can be found for both HA-1 and HA-2 particles that have petal-like surfaces. On the other hand, the needle-like surfaces allow HA-3 particles to have higher specific surface area than both HA-1 and HA-2 particles.

It can be seen from Table 1 that due to the presence of the relatively sparse needle-like surface, HA-3 particles show lower ρ_{bulk} and ρ_{tap} than HA-1 and HA-2 particles. Surface morphology of HA-3 particles allows the particles to have a loose packing. Upon tapping, the needle-like surface packs tightly into each other. Therefore, the difference between ρ_{bulk} and ρ_{tap} is higher for HA-3 particles. The large difference between ρ_{bulk} and ρ_{tap} of the HA-3 particles indicates higher compressibility and poorer flowability than HA-1 and HA-2 particles.

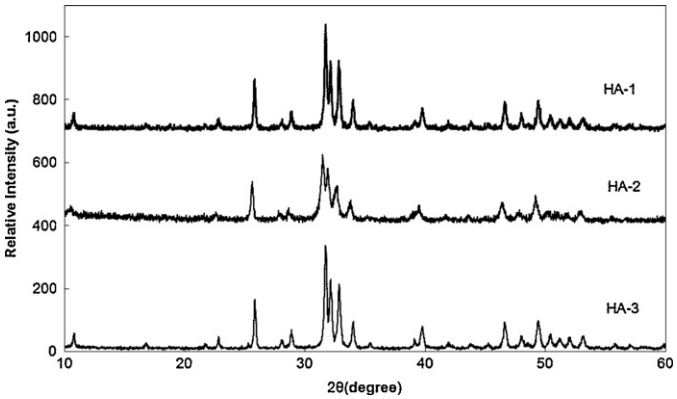

Fig. 3. X-ray diffraction pattern of the pollen-shape carrier particles.

All the three HA samples show similar diffraction patterns in the XRD results illustrated in Fig. 3. A hexagonal phase crystalline structure can be found according to the powder diffraction file (PDF) no. 00-009-0432. The HA particles synthesized in this study can be considered to have high purity. The TGA thermograms of the three HA samples shown in Fig. 4 indicate that there is negligible weight loss (<2%) below 100 °C. The effect of moisture on particle–particle interactions can be neglected for both HA particles (Larhrib et al., 1999).

3.2. Drug blending

Effect of particle size can be obtained by the comparison of HA-1 and HA-2 particles that have similar petal-like surface morphology but have different particle size (d(50%) – 26.6 and 45.9 μm). On the other hand, effect of surface morphology can be obtained by the comparison of HA-1 and HA-3 particles that have similar particle size of 24.8–26.6 μm but different surface morphology. The petal-like surface morphology of HA-1 particles is considered to have dense surface asperities while the needle-like surface morphology of HA-3 particles is considered to have sparse surface asperities.

The model drug, Bd has an average size of 2.5 ± 1.1 μm. Three drug mixing ratios of 2:1, 10:1 and 45:1 (carrier:drug) are used. The physical appearances of the blends are observed in small transparent vials in Fig. 5. Comparison is also made with transparent glass

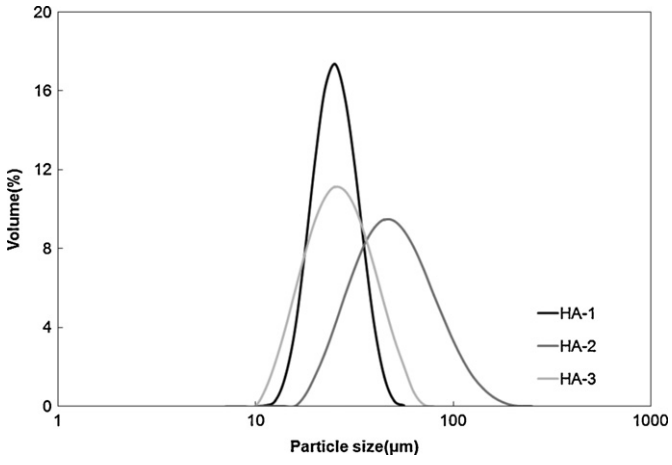

Fig. 2. Size distribution of the pollen-shape carrier particles.

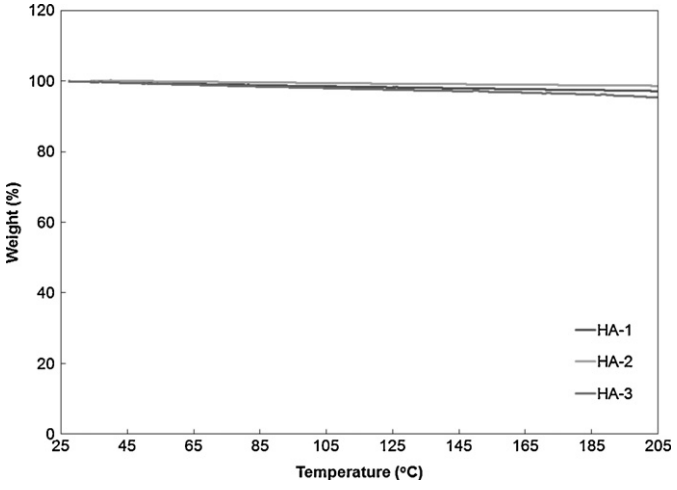

Fig. 4. TGA isotherms of the pollen-shape carrier particles.

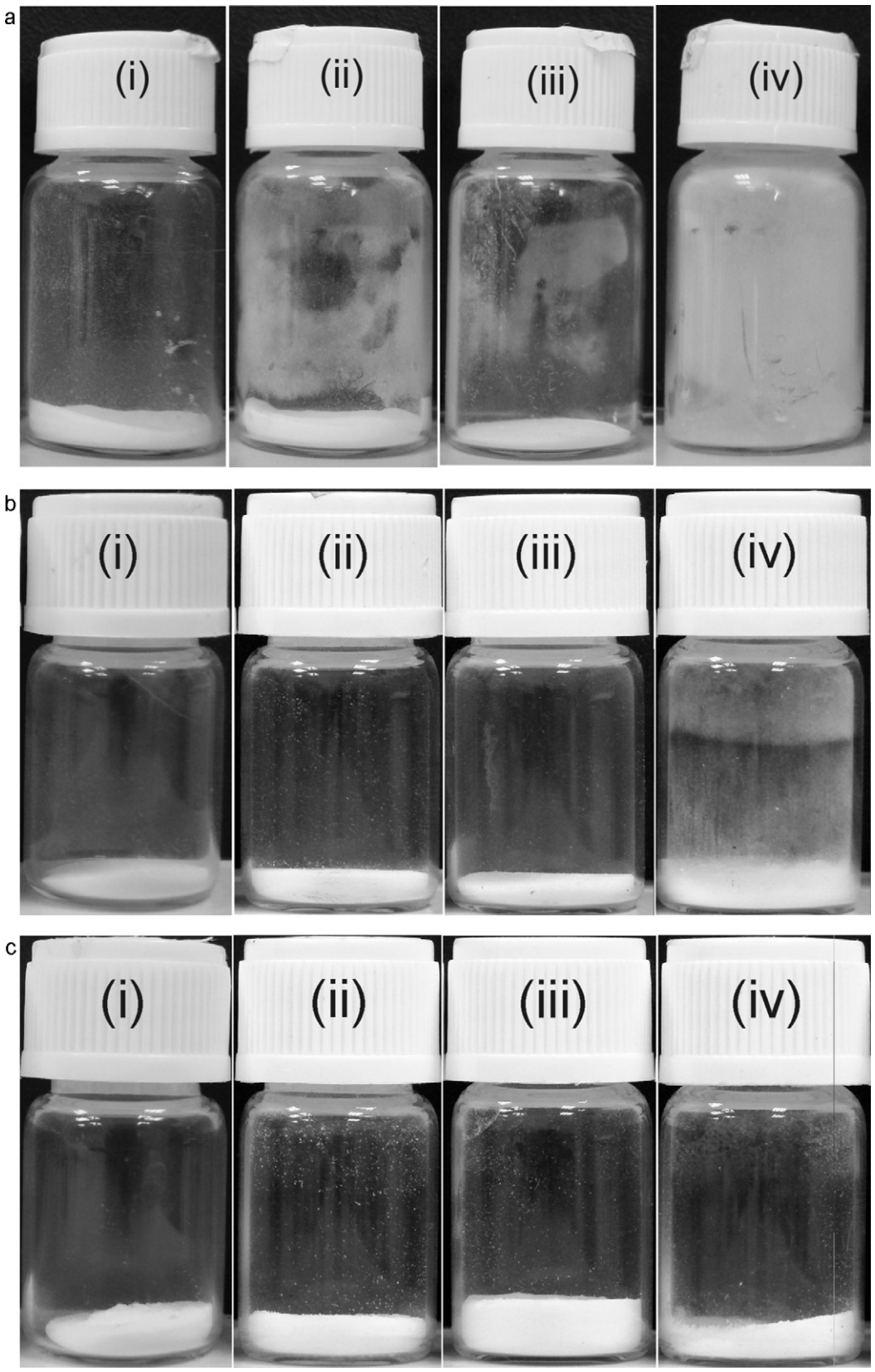

Fig. 5. Comparison of the blends in the mixture vials with (a) HA-1 particles, (b) HA-2 particles, and (c) HA-3 particles, (i) carrier only; (ii) 45:1 (carrier:drug, w/w), (iii) 10:1 (carrier:drug, w/w), and (iv) 2:1 (carrier:drug, w/w).

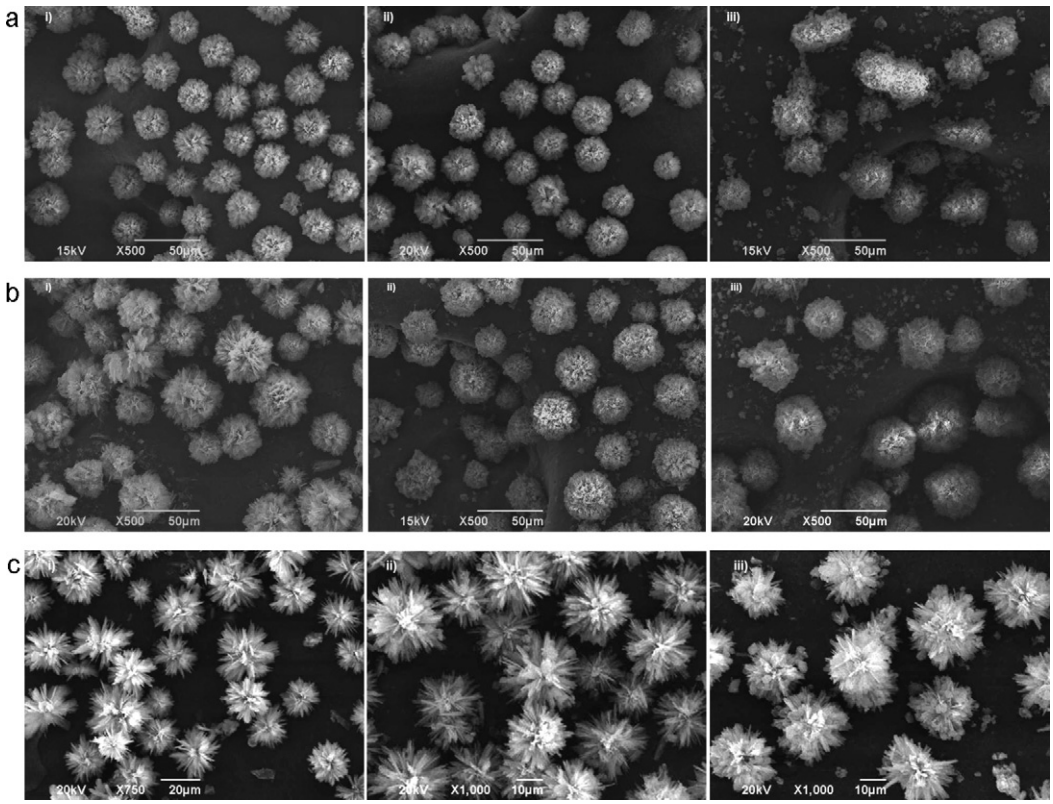

Fig. 6. SEM image of the blends with comparison of the blends, (a) HA-1 particles, (b) HA-2 particles, and (c) HA-3 particles with drug mixing ratios (carrier:drug, w/w), (i) 45:1, (ii) 10:1, and (iii) 2:1.

vials containing the carriers only. As shown in Fig. 5a(i), b(i) and c(i), the vials containing only the carriers show no sign of particle attachment on the vial surface. Thus, the presence of cloudiness on the vial surface is an indication of the attachment of Bd. As the drug mixing ratio increases, the degree of cloudiness on the vial surface increases. It indicates that there is an increasing amount of Bd not being able to attach onto the carriers as the drug mixing ratio increases. A comparison of the vial surfaces between the HA-1 blends and the HA-2 blends shows that HA-2 particles allow better attachment of Bd than HA-1 particles. Even at a high carrier to drug ratio of 2:1, the HA-2 blends show only a minor amount of Bd on the vial surface while the vial containing the HA-1 blends is almost completely covered with Bd. It shows in Table 1 that the specific surface area of HA-1 particles is equivalent to that of HA-2 particles, yet a lower attachment is observed on HA-1 particles. Since the determination of the accessible surface area is not possible, the vial appearance can be used as a qualitative measure of the drug attachment capacity of the carrier particles. When the drug particles are not attached onto the carrier particles properly, the unattached drug particles will be attached to the vial surface and result in a cloudy surface. It can be anticipated that, due to the smaller particle size and denser surface morphology, the accessible surface of HA-1 particles is lower than that of HA-2 particles. Therefore, HA-1 particles may have limited drug attachment capacity.

The vial appearance of the HA-1 blends and the HA-3 blends can be seen in Fig. 5(a) and (c), respectively. As shown in Fig. 5(c), no obvious drug attachment on the vial surface is observed for the HA-3 blends at all drug mixing ratios. The drug particles can be considered to be attached on the surface of the HA-3 particles. As expected from the SEM images, the fairly open surface morphology of HA-3 particles tends to have higher accessible surface area than dense surface morphology of HA-1 particles. As a result, large amount of drug particles can be attached onto the surface of HA-3 particles instead of attaching onto the vial surface.

The vial appearance is a qualitative measure of the drug attachment to the carrier particles but it does not show the inherent characteristics of the drug–carrier attachment. Therefore, the mixtures are also characterized with SEM images. The SEM images for the blends at different drug mixing ratios are shown in Fig. 6. The fine powders at the background of the SEM images can be identified as the unattached Bd. As expected, the amount of unattached Bd increases with an increase in drug mixing ratios. All the three blends show a minor amount of unattached Bd at a carrier to drug ratio of 45:1. Though the difference in drug attachment between the three types of carrier particles are not significant at a carrier to drug ratio of 10:1, it is quite obvious that HA-1 and HA-2 particles has lower drug attachment capacity than HA-3 particles at a carrier to drug ratio of 2:1. It can be anticipated that the needle-like surface morphology is the main contributor to the increase in the drug attachment capacity.

Table 2
Average Bd content and homogeneity of the blends.

Wt ratio (carrier:drug)	Carrier	Wt fraction of drug with carrier (wt%)	CV (%)
2:1	HA-1	20.4	12.73
	HA-2	22.5	0.26
	HA-3	23.7	5.74
10:1	HA-1	8.7	6.91
	HA-2	8.9	2.14
	HA-3	9.0	0.72
45:1	HA-1	1.98	5.70
	HA-2	2.09	6.26
	HA-3	2.16	5.44

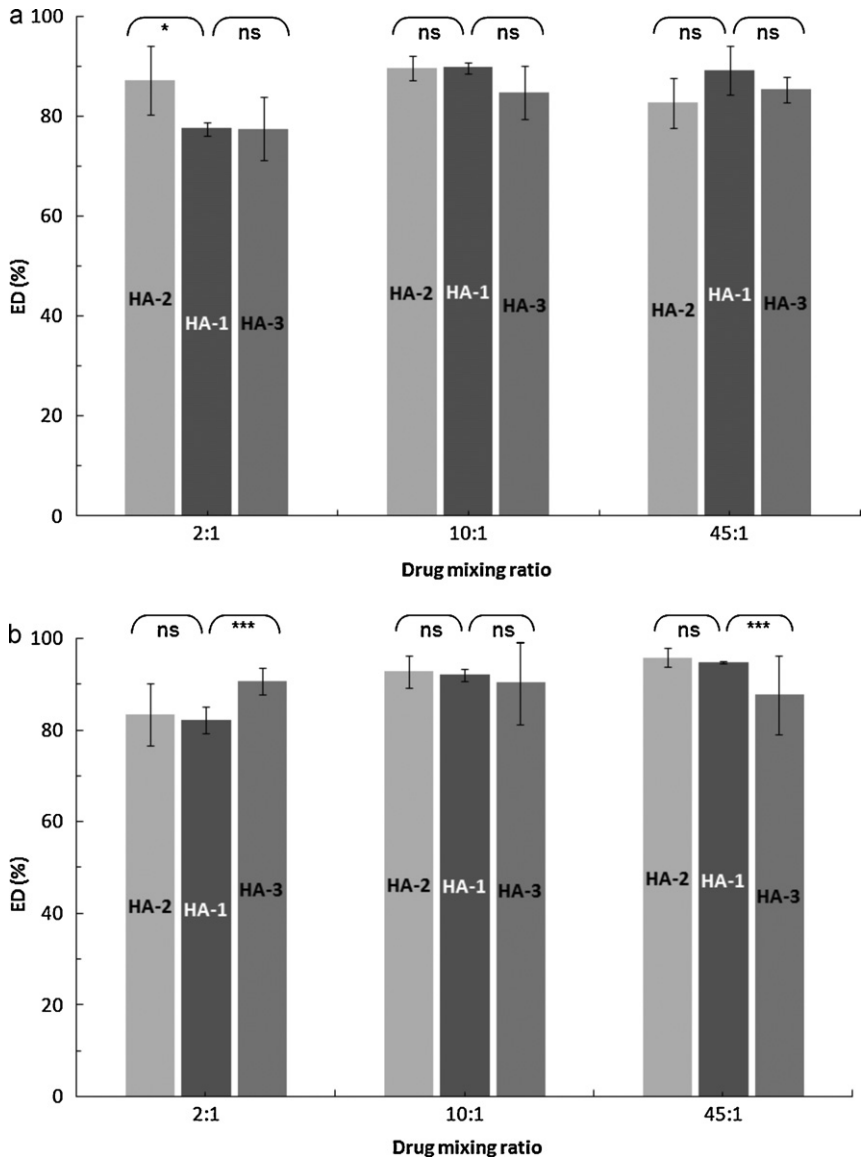

Fig. 7. ED of blends with carrier to drug ratio of 2:1, 10:1 and 45:1 at (a) 30 L/min and (b) 60 L/min ("ns" denotes $p > 0.05$, "*" denotes $p < 0.05$, "**" denotes $p < 0.01$ and "***" denotes $p < 0.001$).

3.3. Blending homogeneity

Blend homogeneity is represented by the coefficient of variance (CV) of the Bd content in the blends. The average drug content and CV for the blends after mixing are listed in Table 2. A comparison in the drug weight fractions between HA-1 and HA-2 particles indicates that an increase in particle size can increase the drug attachment capacity. Even though both HA-1 and HA-2 particles have similar specific surface area, the percentage of the surface that is accessible to Bd will be higher for the larger sized HA-2 particles than HA-1 particles. Similar comparison between HA-1 and HA-3 particles shows that a larger improvement in the drug attachment capacity can be achieved by having a more open surface morphology. Nonetheless, all the blends can be considered as uniform since the CV of the blends are all less than around 10%.

3.4. In vitro aerosolization and deposition behavior

Size and morphology of the carrier particles have significant impact on *in vitro* aerosolization and deposition behavior of the blends. It has been shown that the size and morphology of pollen-shape particles affect the drug attachment capacity. The nature of drug attachment affects the flowability of the blends and the extent of drug liberation, which in turn influences the *in vitro* aerosolization and deposition behavior. The ED and FPF results of the blends are shown in Figs. 7 and 8, respectively. Fisher's least significant difference (LSD) test is applied. Test results are presented in the figures where "ns" denotes $p > 0.05$, "*" denotes $p < 0.05$, "**" denotes $p < 0.01$ and "***" denotes $p < 0.001$.

3.4.1. Effect of particle size and surface morphology on ED

Effect of carrier particle size on ED can be obtained from a comparison of the ED of the HA-1 and HA-2 blends shown in Fig. 7. No significant difference in ED is observed between the HA-1 and HA-2 blends at all conditions except at a high carrier to drug ratio of 2:1 and a low flow rate of 30 L/min. At a carrier to drug ratio of 2:1 and 30 L/min, the HA-2 blend shows a higher ED than the HA-1 blend. As discussed in the earlier section, an increase in carrier particle size increases the accessible surface area for drug attachment per unit weight of carrier particles. At high drug mixing ratios, the excess drug particles that are not attached to the carrier particles tend to form aggregates. While a flow rate of 30 L/min is not sufficient

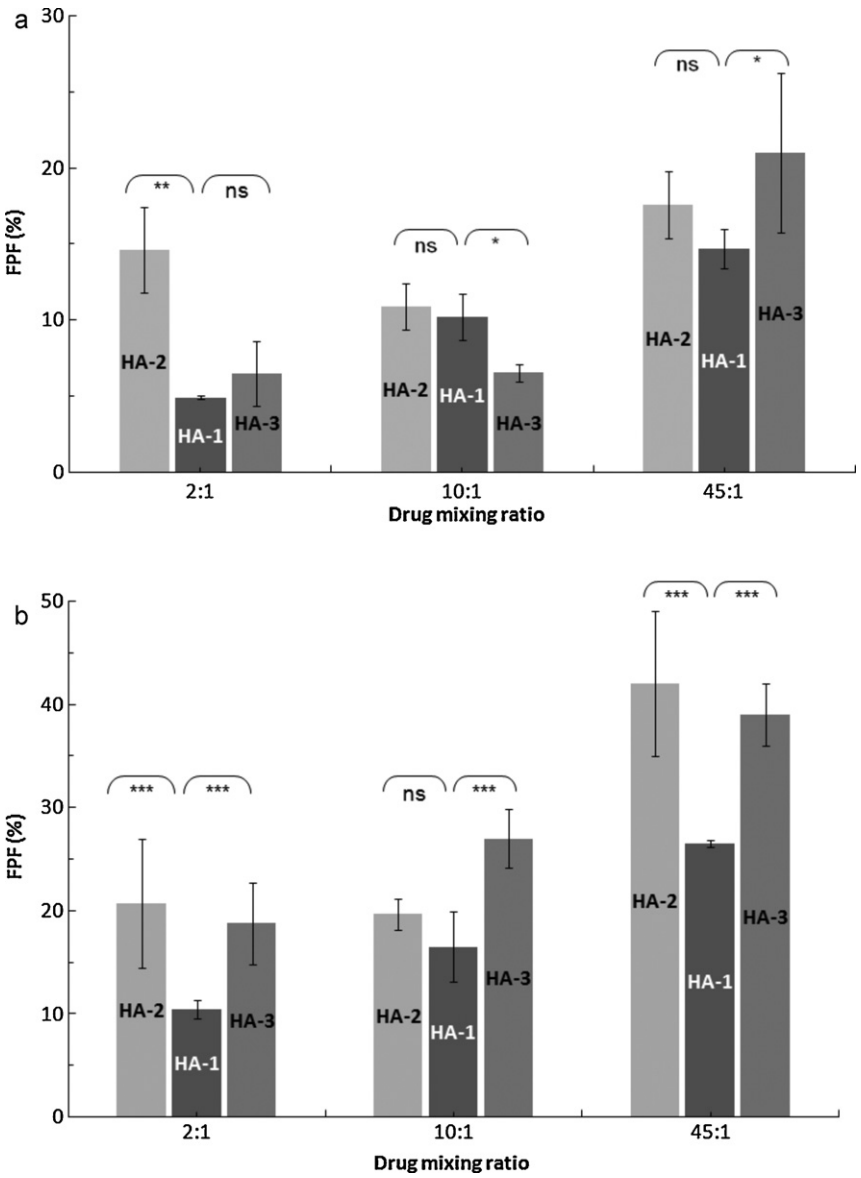

Fig. 8. FPF of blends with carrier to drug ratio 2:1, 10:1 and 45:1 at (a) 30 L/min and (b) 60 L/min ("ns" denotes $p > 0.05$, "*" denotes $p < 0.05$, "**" denotes $p < 0.01$ and "***" denotes $p < 0.001$).

to disperse the aggregates, the aggregates tend to remain in the inhaler and cause a reduction in ED. Therefore, it can be anticipated that an increase in carrier particle size improves the ED only when the drug mixing ratio exceeds the capacity of the carrier particles and the flow rate is not sufficient to disperse the drug aggregates.

A comparison of the ED of the HA-1 and HA-3 blends shown in Fig. 7 reveals the effect of carrier particle surface morphology on ED. The HA-1 blends are found to have slightly higher EDs compared to the HA-3 blends at low drug mixing ratios and low flow rate though the differences are considered insignificant. However, the EDs of the HA-3 blends become equivalent or better than that of the HA-1 blends when the drug mixing ratio and/or flow rate is increased. A comparison of the bulk and tap densities of HA-1 and HA-3 particles in Table 1 shows that HA-3 particles have poorer flowability than HA-1 particles (Hassan and Lau, 2010a). It is more difficult to disperse the HA-3 blends at low drug mixing ratios at a flow rate of 30 L/min. On the other hand, HA-3 particles have higher specific surface area than HA-1 particles. Based on the discussion of the vial appearance in the earlier section, HA-3 particles are found to have a higher drug attachment capacity than HA-1 particles for the same particle size. Therefore, the high drug attachment capacity of HA-3 particles becomes increasingly important at higher drug mixing ratios. In addition, the dispersion of HA-3 particles becomes equivalent to HA-1 particles at a flow rate of 60 L/min. The drug attachment capacity becomes the dominating factor particular when the drug mixing ratio is approaching the capacity limits of the carrier particles. Thus, the HA-3 blends eventually have higher ED than the HA-1 blends at a carrier to drug ratio of 2:1 and flow rate of 60 L/min. Carrier particles having sparse surface asperities improve the drug attachment capacity but lower the flowability compared to those having dense surface asperities. The two counteracting factors favor the use of dense surface carrier particles at low drug mixing ratio and low flow rates while the use of sparse surface carrier particles are more favorable at high drug mixing ratio and high flow rates to improve the ED.

3.4.2. *Effect of particle size and surface morphology on FPF*

The FPF results of the HA-1 and HA-2 blends are shown in Fig. 8. All the HA-2 blends show equivalent or better FPF than the HA-1 blends under the same conditions. The difference is the most obvi-

ous at a high carrier to drug ratio of 2:1 and a flow rate of 60 L/min. It is discussed in the previous sections that HA-1 particles have lower accessible surface area for drug attachment per unit weight of carrier particles compared to HA-2 particles. When the drug mixing ratio is below the capacity of the carrier particles, both HA-1 and HA-2 particles behave in a similar manner. The slightly better FPF of the HA-2 blends maybe a direct reflection of the better flowability compared with the HA-1 blends. The difference in drug attachment capacity becomes the dominating factor when the drug mixing ratio is high. Thus, the HA-2 blends outperforms the HA-1 blends at a carrier to drug ratio of 2:1. In addition, the use of a high flow rate has a twofold effect on the FPF of the blends. On one hand, a high flow rate allows an improvement in the dispersion of the drug particles even if they are in aggregate form. The high flow rate also improves the detachment of drug particles from the carrier surfaces after the dispersion. The combined effect of an improved drug detachment and a high ED thus causes the HA-2 blends to have significantly higher FPF than the HA-1 blends at high drug mixing ratio and high flow rate conditions. For pollen-shape carrier particles, an increase in the particle size is advantageous to the improvement of the FPF.

A comparison of the FPFs of the HA-1 and HA-3 blends in Fig. 8 shows that no definite conclusion can be drawn about the effects of carrier surface morphology on FPF at a flow rate of 30 L/min. However, a flow rate of 60 L/min allows the HA-3 blends to have significantly higher FPF than the HA-1 blends at all drug mixing ratios. Since the differences in ED between the HA-1 and HA-3 blends at a flow rate of 60 L/min vary to a certain degree, detailed analysis of the relations between the EDs and the FPFs is necessary. Despite the fact that ED of the HA-3 blends at 60 L/min and low drug loading is smaller than that of the HA-1 blends, the HA-3 blends have higher FPF than the HA-1 blends. It is reasonable to assume that the difference in drug attachment capacity between HA-1 and HA-3 particles can be disregarded when the drug mixing ratio is low. The poorer flowability of HA-3 particles than HA-1 particles, in this case, should suggest the opposite of the observed results. Therefore, it is anticipated that there is additional factor in the sparse asperities of HA-3 particles serving to improve the FPF. Further comparison of the physical properties of HA-1 and HA-3 particles in Table 1 reveals that HA-3 particles have significantly lower tap and bulk densities than HA-1 particles. It is known that particle aerodynamic diameter is proportional to the square root of the particle density. Therefore, HA-3 particles are anticipated to have a smaller aerodynamic diameter than HA-1 particles. With a smaller aerodynamic diameter, HA-3 particles are able to deliver even the un-detached drug particles to the lower stages to achieve a high FPF.

4. Conclusion

The drug delivery performance of three types of pollen-shape carrier particles having various size and surface morphology are investigated at various drug mixing ratios and flow rates. It is found that an increase in carrier particle size increases the accessible surface area per unit weight of the carrier particles. An improvement in the drug attachment capacity can improve the ED at high drug mixing ratios and low flow rates while no substantial effect at low drug mixing ratios or high flow rate conditions. However, a large carrier particle size significantly improves the FPF particularly at high drug mixing ratio and high flow rate conditions. A sparse carrier surface asperity is found to have better drug attachment capacity than a dense carrier surface asperity. However, no significant effect of surface asperity on ED is observed at low flow rates. At high flow rates, the high attachment capacity and the reduced aerodynamic diameter of carrier particles having a sparse surface asperity allow a better FPF than carrier particles having a dense surface asperity.

Acknowledgement

The authors are grateful to the financial support of AcRF Tier1 Grant, RG 14/09.

References

Begat, P., Morton, D.A.V., Staniforth, J.N., Price, R., 2004. The cohesive–adhesive balances in dry powder inhaler formulations. II. Influence on fine particle delivery characteristics. Pharm. Res. 21, 1826–1833.
Broadhead, J., Rouan, S., Hau, I., Rhodes, C., 1994. The effect of process and formulation variables on the properties of spray-dried beta-galactosidase. J. Pharm. Pharmacol. 46, 458–467.
Dolovich, M.B., 2001. Measuring total and regional lung deposition using inhaled radiotracers. J. Aerosol Med. 14, 35–44.
Flament, M.-P., Leterme, P., Gayot, A., 2004. The influence of carrier roughness on adhesion, content uniformity and the *in vitro* deposition of terbutaline sulphate from dry powder inhalers. Int. J. Pharm. 275, 201–209.
French, D.L., Edwards, D.A., Niven, R.W., 1996. The influence of formulation on emission, deaggregation and deposition of dry powders for inhalation. J. Aerosol Sci. 27, 769–783.
Gonda, I., 1996. Scintigraphic techniques for measuring *in vivo* deposition. J. Aerosol Med. 9, S 59–S 67.
Gonda, I., 2004. Targeting by deposition. In: Hicky, A.J. (Ed.), Pharmaceutical Inhalation Aerosol Technology. Marcel Dekker, Inc., New York.
Guchardi, R., Frei, M., John, E., Kaerger, J.S., 2008. Influence of fine lactose and magnesium stearate on low dose dry powder inhaler formulations. Int. J. Pharm. 348, 10–17.
Hassan, M.S., Lau, R., 2010a. Feasibility study of pollen-shape drug carriers in dry powder inhalation. J. Pharm. Sci. 99, 1309–1321.
Hassan, M.S., Lau, R., 2010b. Flow behavior and deposition study of pollen-shape carrier particles in an idealized inhalation path model. Particuology 8, 51–59.
Hassan, M.S., Lau, R., 2010c. Inhalation performance of pollen-shape carrier in dry powder formulation with different drug mixing ratios: comparison with lactose carrier. Int. J. Pharm. 386, 6–14.
Heng, P.W.S., Chan, L.W., Lim, L.T., 2000. Quantification of the surface morphologies of lactose carriers and their effect on the *in vitro* deposition of salbutamol sulphate. Chem. Pharm. Bull. 48, 393–398.
Iida, K., Hayakawa, Y., Okamoto, H., Danjo, K., Leuenberger, H., 2001. Evaluation of flow properties of dry powder inhalation of salbutamol sulfate with lactose carrier. Chem. Pharm. Bull. 49, 1326.
Iida, K., Hayakawa, Y., Okamoto, H., Danjo, K., Luenberger, H., 2004. Influence of storage humidity on the *in vitro* inhalation properties of salbutamol sulfate dry powder with surface covered lactose carrier. Chem. Pharm. Bull. 52, 444–446.
Islam, N., Stewart, P., Larson, I., Hartley, P., 2004. Effect of carrier size on the dispersion of salmeterol xinafoate from interactive mixtures. J. Pharm. Sci. 93, 1030–1038.
Kassem, N.M., Ganderton, D., 1990. The influence of carrier surface on the characteristics of inspirable powder aerosols. J. Pharm. Pharmacol. 42, 11P.
Kawashima, Y., Serigano, T., Hino, T., Yamamoto, H., Takeuchi, H., 1998. Effect of surface morphology of carrier lactose on dry powder inhalation property of pranlukast hydrate. Int. J. Pharm. 172, 179–188.
Larhrib, H., Cespi, M., Dyas, M.A., Roberts, M., Ford, J.L., 2006. Engineered carrier with a long time of flight (TOF) to improve drug delivery from dry powder inhalation aerosols. Drug Deliv. Lung (DDL), 304–307.
Larhrib, H., Martin, G.P., Marriott, C., Prime, D., 2003a. The influence of carrier and drug morphology on drug delivery from dry powder formulations. Int. J. Pharm. 257, 283–296.
Larhrib, H., Martin, G.P., Prime, D., Marriott, C., 2003b. Characterisation and deposition studies of engineered lactose crystals with potential for use as a carrier for aerosolised salbutamol sulfate from dry powder inhalers. Eur. J. Pharm. Sci. 19, 211–221.
Larhrib, H., Zeng, X.M., Martin, G.P., Marriott, C., Pritchard, J., 1999. The use of different grades of lactose as a carrier for aerosolised salbutamol sulphate. Int. J. Pharm. 191, 1–14.
Li, Q., Rudolph, V., Peukert, W., 2006. London-van der Waals adhesiveness of rough particles. Powder Technol. 161, 248–255.
Li, Q., Rudolph, V., Weigl, B., Earl, A., 2004. Interparticle van der Waals force in powder flowability and compactibility. Int. J. Pharm. 280, 77–93.
Louey, M., Van Oort, M., Hickey, A., 2004a. Aerosol dispersion of respirable particles in narrow size distributions produced by jet-milling and spray-drying techniques. Pharm. Res. 21, 1200–1206.
Louey, M., Van Oort, M., Hickey, A., 2004b. Aerosol dispersion of respirable particles in narrow size distributions using drug-alone and lactose-blend formulations. Pharm. Res. 21, 1207–1213.
Louey, M.D., Razia, S., Stewart, P.J., 2003. Influence of physico-chemical carrier properties on the *in vitro* aerosol deposition from interactive mixtures. Int. J. Pharm. 252, 87–98.
Mumenthaler, M., Hsu, C.C., Pearlman, R., 1994. Feasibility study on spray-drying protein pharmaceuticals: recombinant human growth hormone and tissue-type plasminogen activator. Pharm. Res. 11, 12–20.
Niven, R.W., Lott, F.D., Ip, A.Y., Cribbs, J.M., 1994. Pulmonary delivery of powders and solutions containing recombinant human granulocyte colony-stimulating factor (rhG-CSF) to the rabbit. Pharm. Res. 11, 1101–1109.

Philip, V.A., Mehta, R.C., Mazumder, M.K., DeLuca, P.P., 1997. Effect of surface treatment on the respirable fractions of PLGA microspheres formulated for dry powder inhalers. Int. J. Pharm. 151, 165–174.

Podczeck, F., 1999. The influence of particle size distribution and surface roughness of carrier particles on the *in vitro* properties of dry powder inhalations. Aerosol Sci. Technol. 31, 301–321.

Shi, L., Plumley, C.J., Berkland, C., 2007. Biodegradable nanoparticle flocculates for dry powder aerosol formulation. Langmuir 23, 10897–10901.

Singh, M., Waluch, V., 2000. Physics and instrumentation for imaging in-vivo drug distribution. Adv. Drug Deliv. Rev. 41, 7–20.

Srichana, T., Martin, G.P., Marriott, C., 1998. On the relationship between drug and carrier deposition from dry powder inhalers *in vitro*. Int. J. Pharm. 167, 13–23.

Steckel, H., Müller, B.W., 1997. *In vitro* evaluation of dry powder inhalers. II. Influence of carrier particle size and concentration on in vitro deposition. Int. J. Pharm. 154, 31–37.

Visser, J., 1989. Van der Waals and other cohesive forces affecting powder fluidization. Powder Technol. 58, 1–10.

Wang, Y., Hassan, M.S., Gunawan, P., Lau, R., Wang, X., Xu, R., 2009. Polyelectrolyte mediated formation of hydroxyapatite microspheres of controlled size and hierarchical structure. J. Colloid Interface Sci. 339, 69–77.

Young, P.M., Edge, S., Traini, D., Jones, M.D., Price, R., El-Sabawi, D., Urry, C., Smith, C., 2005. The influence of dose on the performance of dry powder inhalation systems. Int. J. Pharm. 296, 26–33.

Zeng, X.-M., Martin, G.P., Marriott, C., Pritchard, J., 2001. Lactose as a carrier in dry powder formulations: the influence of surface characteristics on drug delivery. J. Pharm. Sci. 90, 1424–1434.

Zeng, X.M., Martin, G.P., Marriott, C., Pritchard, J., 2000. The influence of carrier morphology on drug delivery by dry powder inhalers. Int. J. Pharm. 200, 93–106.

Zeng, X.M., Martin, G.P., Tee, S.-K., Ghoush, A.A., Marriott, C., 1999. Effects of particle size and adding sequence of fine lactose on the deposition of salbutamol sulphate from a dry powder formulation. Int. J. Pharm. 182, 133–144.